Robust estimation of axial loads sustained by tie-rods in historical structures using Artificial Neural Networks

Nirvan Makoond[1], Luca Pelà[2] and Climent Molins[2]

Abstract

Widely used simplified analytical methods for estimating the tensile force in tie-rods are clearly not applicable when they contain significant discontinuities or irregularities. A common example for which this fact becomes relevant in practice is the use of connectors to unify historical ties consisting of several segments. To address this challenge, a robust hybrid methodology is proposed which can be applied to any historical tie by employing a data-driven approach to a dataset generated using the finite element method. The methodology is applied to a real case study involving two historical ties.

Keywords

Axial force estimation, Vibration testing, Dynamic identification, Modal Analysis, Natural frequency, Mode shapes

Introduction

Tie-rods have and are still commonly used in historical masonry constructions to counteract lateral thrusts, most often imposed by vaults or arches. They can contribute significantly to structural equilibrium and their effectiveness is usually directly related to the magnitude of the tensile load they sustain. This load can vary significantly over time due to phenomena such as steel relaxation, corrosion damage, differential settlements and support spreading, among others[1]. As such, knowledge of the actual axial load in a tie-rod is often a crucial piece of information required for adequate structural safety assessment. It should therefore come as no surprise that the development of experimental methods for the accurate estimation of this quantity has received considerable attention from the scientific community in the past[2–18].

At the broadest level, it can be said that there are two types of experimental methods that may be employed to estimate the axial force in tie-rods: direct and indirect. The direct approach involves gradually releasing the tension in a tie-rod until the axial stress is eliminated while using strain gauges to measure the pre-existing axial deformation. Knowledge of the geometric characteristics of the tie-rod and elastic properties of its material can then be used with these measurements to infer the actual tensile load. Naturally, this method is not applicable in many cases, either because the ends

of a tie-rod cannot be loosened (due to the type of anchor itself or due to poor condition), or because the release of the axial load in the tie-rod could compromise structural safety. As such, the present study and most of the research performed over the past 4 decades focuses exclusively on indirect methods.

Indirect methods may be further categorised as static or dynamic. Static methods involve measuring vertical displacements (and strains) after imposing specific loads on a tie-rod, whereas dynamic approaches involve recording acceleration time-histories of the tie and extracting modal parameters such as natural frequencies and corresponding mode shape amplitudes. The axial load can then be inferred from these experimentally determined parameters using a suitable mathematical model of the tie. Although the problem of determining the axial load from the aforementioned measurements may at first seem trivial, the case of historic ties anchored in masonry walls is typically characterised by significant uncertainty on the nature of the actual boundary conditions[15]. These often lie somewhere in

[1]ICITECH, Universitat Politècnica de València, Valencia, Spain
[2]Department of Civil and Environmental Engineering, Universitat Politècnica de Catalunya (UPC-BarcelonaTech), Barcelona, Spain

Corresponding author:
Nirvan Makoond, ICITECH Universitat Politècnica de València, Camino de Vera s/n, 46022 Valencia, Spain.
Email: ncmakoon@upv.es

between fully pinned end restraints and fully fixed ones, allowing a certain limited degree of rotation. Of course, end constraints influence both the static and dynamic response of the ties and in many cases, the effect of the a priori uncertainty of end conditions on the observed natural frequencies or deformations can be larger than the effect of different axial load levels. In some cases, uncertainties on the effective elastic modulus, on the regularity of cross-sections, or on the straightness of the bar can also have some effects on measured parameters, but these are usually much less significant. To deal with some of these challenges, most notably with the case of uncertain boundary conditions, several different indirect methods have been developed over the years (see Table 1), each having their own advantages and disadvantages in terms of accuracy, applicability and difficulty of the experimental procedure.

Among the model unknowns listed in Table 1, N refers to the axial load, while k_L and k_R refer to the rotational spring stiffnesses from the model shown in Fig. 1(a). The model considered by Li et al.[12] additionally includes two vertical translational springs at each end with stiffnesses of $k_{T,l}$ and $k_{T,r}$. M_A and M_B refer to bending moments at either end of a section of a tie instrumented with strain gauges placed on the upper surface (measuring $\epsilon_{x,u}$) and the lower one (measuring $\epsilon_{x,l}$). $\boldsymbol{K_A}$ and $\boldsymbol{K_B}$ each refer to a 2×2 matrix containing the stiffness parameters of a set of elastic springs considered by a reference model of an instrumented section of a tie. E is the elastic modulus of the tie's material and ρ its density, while J is the second moment of area of the tie's cross-section. L and l_f refer to the lengths shown in Fig. 1 and m_{cen} to the central lumped mass considered in the model proposed by Garziera et al.[10]. With respect to required experimental parameters, Δ_z refers to the vertical displacement of a tie measured under the effect of a concentrated load imposed during a static test. f_n and Δ_M refer respectively to the frequency of a natural mode of vibration of a tie and any component of the corresponding mode shape vector, identified from acquisitions made during dynamic tests. It should be mentioned that all the previous methods presented in Table 1 consider the tie as a beam with at least flexural rigidity. Additionally, some of the methods use a model which also considers shear deformations according to the Timoshenko beam theory. Earlier methods were based on a vibrating wire model that neglects the flexural rigidity of the tie[19].

The vast majority of these methods rely on one of the two idealisations of a tie-rod shown in Fig. 1. The model shown in Fig. 1(a) consists of a tie-rod with length L equal to the free span between the interior surfaces of the two walls where the tie is anchored. In this idealisation, the tie is modelled as a simply supported beam sustaining an axial load N with rotational springs at either end (with stiffnesses of k_L and k_R). Fig. 1(b) shows a tie-rod modelled as a simply supported beam with elastic Winkler foundations used to simulate the interaction between the beam and walls. The Winkler foundations with stiffness k_f are assumed to be acting over the length l_f corresponding to the portion of the beam inserted in the wall on either side.

In fact, most of the reviewed methods summarised in Table 1 rely on the model presented in Fig. 1(a). Specifically, the methods presented in[2,3,5–8,11,14] rely on this model. The model considered in[12] also considers two vertical translational springs at either end in addition to the rotational ones. To the best of the authors' knowledge, the model shown in Fig. 1(b) was first proposed by Amabili et al.[9]. A modified version of this model, which simply considers an additional lumped mass in the centre of the beam (indicated with a dotted line in Fig.1(b)), was proposed by Garziera et al.[10] to deal with the special case of tie-rods consisting of a central connector unifying two separate rod sections.

Besides the methods employed in[9,10,12], only those proposed by Bati & Tonietti[4] and Rebecchi et al.[13] are not based on one of the models shown in Fig. 1. The models used as a basis for both these methods only consider an instrumented section of the length of the tie instead of the whole length from end-to-end. As such, both these models do not require knowledge of the tie length which can be characterised by significant uncertainty stemming from the interaction between the walls on either end and the tie-rod itself. Nevertheless, since both these models do not consider the actual tie ends, they cannot produce results on the stiffness of the ends that can be readily interpreted. Apart from this specific difference, the basic models employed by these two methods are in fact very similar to that shown in Fig. 1(a), consisting of an axially loaded member with flexural rigidity and unknown moments or equivalent elastic spring stiffnesses at either end of the considered section.

Despite the fact that some experimental studies performed under laboratory conditions show that the static method proposed by Bati & Tonietti can lead to

Table 1. Existing indirect methods for estimating the axial load in tie-rods.

Authors and year	Type of approach	Required experimental parameters (Inputs)	Model unknowns	Estimates obtained (Outputs)
Beconcini (1996)[2]	Static	Δ_z at 3 locations	$N, k_\theta = k_L = k_R$	All 2 unknowns
Blasi & Sorace (1994)[3]	Mixed	Δ_z at mid-span & fundamental f_n	N, k_θ	All 2 unknowns
Bati & Tonietti (2001)[4]	Static	Δ_z at 3 locations; $\epsilon_{x,u}$ & $\epsilon_{x,l}$ at 3 locations	N, M_A, M_B	All 3 unknowns
Dardano et al. (2005)[5]	Dynamic	Two different f_n	N, k_θ	All 2 unknowns[†]
Lagomarsino & Calderini (2005)[6]	Dynamic	Three different f_n	N, k_θ, EJ	All 3 unknowns
Park et al. (2005)[7]	Dynamic	As many f_n as can be captured	N, k_θ	All 2 unknowns[†]
Tullini & Laudiero (2008)[8]	Dynamic	f_n & corresponding Δ_M at 3 locations	N, k_L, k_R	All 3 unknowns
Amabili et al. (2010)[9]	Dynamic	As many f_n as can be captured	N, k_f	All 2 unknowns[†]
Garziera et al. (2011)[10]	Dynamic	As many f_n as can be captured	N, k_f, L, l_f, m_{cen}	All 5 unknowns[†]
Gentilini et al. (2012)[11]	Dynamic	First 4 f_n under different conditions*	N, k_L, k_R, E	All 4 unknowns
Li et al. (2012)[12]	Dynamic	f_n & corresponding Δ_M at 5 locations	$N, k_L, k_R, k_{T,l}, k_{T,r}$	All 5 unknowns
Rebecchi, Tullini & Laudiero (2013)[13]	Dynamic	f_n & corresponding Δ_M at 5 locations	$N, \boldsymbol{K_A}, \boldsymbol{K_B}$	N
Campagnari et al. (2017)[14]	Dynamic	2nd, 3rd & 4th f_n & corresponding Δ_M at 2 locations	N, k_L, k_R, L, E, ρ	All unknowns

* The first 4 f_n need to be evaluated under the effect of a concentrated load placed at least in one position.

† Although the complete solution is only provided for the case of equal stiffnesses at either end in the corresponding publications, the methods can in theory be extrapolated to consider a different stiffness at the right and left ends.
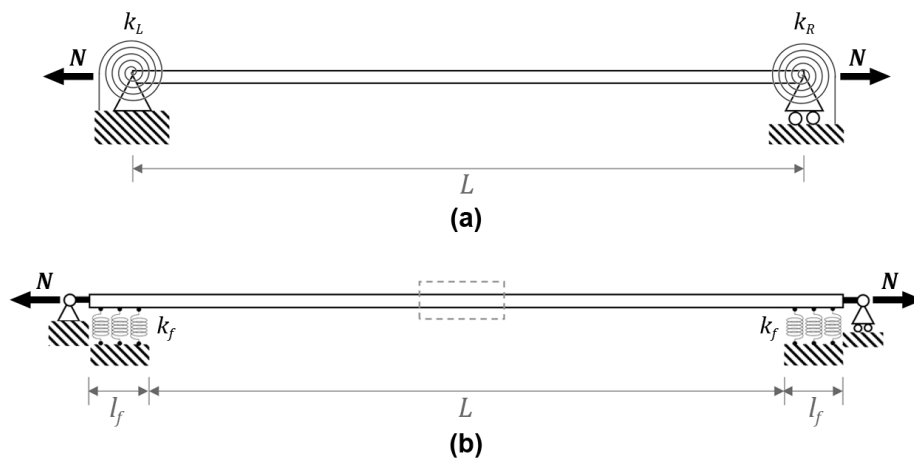

Figure 1. Reference tie-rod models employed by most indirect methods: (a) tie-rod modelled as a simply supported beam, (b) tie-rod modelled as a simply supported beam with elastic Winkler foundations used to simulate the interaction between the beam and walls.

more accurate results compared to some of the dynamic methods[20], it is clear that the scientific community has focused more on the development of dynamic methods over the last decade (see Table 1). First and foremost, this is most probably due to the greater effort that the static experimental procedures require. Specifically, they involve imposing concentrated loads at specific points along the length of the tie and measuring longitudinal strains as well as vertical deflections. All of these tasks can prove to be challenging and very

time-consuming, particularly for ties placed at great heights. In addition, estimates from static methods can be particularly sensitive to small experimental errors which the testing procedures are particularly susceptible to (e.g: errors in strain measurement).

With respect to previously proposed dynamic indirect methods, it can be said that they can be further subdivided into two main categories. The first includes methods proposed in [5,8,12,13] and involve the direct solution of a particular analytical model based on experimentally measured inputs. The approach used in [5] only employs natural frequencies as inputs and therefore imposes no specific constraints on the experimental procedure. On the other hand, the methods used in [8,12,13] also employ components of a mode shape vector as inputs, and therefore require a certain number of sensors placed at specific locations. The second category includes methods proposed in [6,7,9–11] and basically involve an iterative procedure to minimise the error between experimentally identified natural frequencies and those predicted by a set of theoretical or numerical models. The method proposed by Campagnari et al.[14] extends this concept by including an error minimisation task within a systematic model updating procedure.

Clearly, the aforementioned methods that are based on analytical models of a tie with a uniform cross-section cannot be directly applied to cases when ties contain discontinuities or significant irregularities. A common example for which this fact becomes relevant in practice is the use of connectors to unify historical ties consisting of several segments. On the other hand, such irregularities can naturally be considered in methods based on minimising the error between natural frequencies predicted by finite-element (FE) simulations and experimentally observed ones. However, in doing so, these methods do not allow useful information on the mode shapes to be considered in the estimation of the axial load, even if it has been acquired experimentally. This can be a significant limitation, given that the usefulness of mode shape components is clearly demonstrated by the proven accuracy of some of the analytical model-based methods for ties with a continuous regular cross-section [8,20,21].

Besides the ones based only on natural frequency error minimisation, all the reviewed existing methods employ an experimental procedure requiring the positioning of sensors in very specific locations. This can become an important limitation for certain cases, particularly for ties with significant irregularities or discontinuities. For instance, some methods could require the placing of sensors in locations whereby the vibration is influenced by a significant irregularity.

In general, a review of the exiting methods proposed in literature appears to reveal that all of them suffer from at least one of the following limitations:

- Not applicable for the case of ties with irregularities or discontinuities.

- Experimental procedure cannot be adapted to the specific constraints of a particular case.

- Methodology cannot be adapted to fully take advantage of the useful information that could be obtained experimentally.

Artificial Neural Networks (ANN) offer a promising possibility for developing a methodology able to overcome these limitations because they are essentially a programming paradigm that enables a computer to learn from observational data [22]. This is particularly true today due to current capabilities to easily generate accurate data sets of observable parameters for a range of different situations using numerical simulations. In fact, there are several examples of successful applications of ANNs and other machine learning (ML) techniques to extract useful information from images or from data acquired using structural health monitoring (SHM) systems installed in heritage structures [23,24]. Some of these methods have even been used for damage identification or model updating based on the acquired vibration signatures of a structure [24,25]. However, to the best of the authors' knowledge, there exists no methods proposed in literature that employ ANNs to estimate the axial load in tie-rods from data acquired during dynamic tests.

As such, this research aims to develop a novel methodology, employing ANNs, to estimate the actual axial load in historical ties from vibration measurements. In particular, this methodology should be able to overcome the aforementioned limitations of existing methods.

A very brief overview of relevant aspects of ANNs is first given before presenting the proposed methodology. An application to the real case study of two historical ties made up of several segments joined together by large connectors is then presented before discussing the final conclusions.
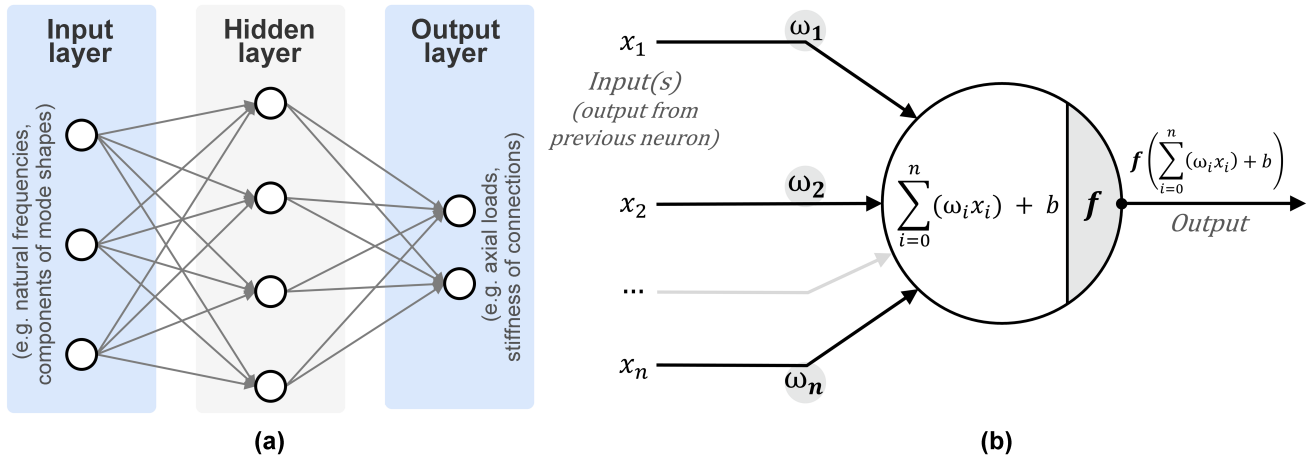
Figure 2. (a) Basic example of a feedforward Artificial Neural Network. (b) Processing performed by neurons.

Artificial Neural Networks (ANNs)

Artificial Neural Networks (ANNs) are a family of biologically-inspired machine learning algorithms that have found widespread applications in a diverse range of fields. Due to the context in which they are being used, ANNs will only be discussed with respect to regression problems in this article. However, it should be noted that they may also be employed for classification and density estimation problems[26]. Providing an extensive and comprehensive overview of ANNs is beyond the scope of this article but there exist many references that can be consulted for this purpose[22,27]. Nevertheless, the basic functionality and the most key aspects of feedforward neural networks, one of the simplest types of ANN, will be described in this section because this information is necessary for understanding the proposed methodology to estimate the axial load in historical ties from vibration records.

The fundamental purpose of a feedforward ANN is to learn relationships between a set of independent variables, which serve as inputs to the network, and a set of dependent variables, designated as the outputs of the network. Following this learning process, the ANN can be used to predict outputs from new input data. Feedforward ANNs consist of an input layer, a number of hidden layers, and an output layer, all made up of a number of processing nodes often referred to as neurons. The number of neurons in the input and output layers rely entirely on the formulation of the problem and the nature of the data. Specifically, the number of chosen inputs and outputs correspond to the number of neurons in these respective layers.

An example of the architecture of a very simple feedforward ANN with a single hidden layer is shown in Fig. 2(a), while the basic processing performed in every neuron is shown in Fig. 2(b). As shown, each input (x_i) fed into a neuron is multiplied by a corresponding weight (ω_i) and a bias (b) is added to the sum of all these products for a particular neuron before passing the result through a specific function commonly referred to as the activation function. The resulting output is then passed on as inputs to the neurons of the next layer. The fundamental process which allows ANNs to learn from input-output data is known as training, and broadly refers to the optimisation of all the weight and bias variables of a given network in order to minimise a suitable loss function, which is a previously defined error metric between predicted and actual outputs. This is achieved by first computing the partial derivatives of the loss function with respect to each weight and bias using an algorithm known as backpropagation. These expressions tell us how quickly the loss function changes when different weights and biases are changed. An iterative optimisation algorithm can then be used to find an optimal combination of weights and biases corresponding to a minimum point of the loss function, i.e minimising the error metric. Every complete iteration using all the training data to compute a new configuration of weights and biases is known as an epoch. Naturally, given the iterative nature of optimisation algorithms, they are susceptible to converge at a local minimum rather than a global one. Several factors influence this susceptibility: from the number of hidden layers, which changes the shape of the feature space being minimised, to specific characteristics of the chosen optimisation algorithm itself. These factors will not be discussed further in this article but extensive descriptions of the most significant ones are available in the book by Hagan et al.[27]. Since

the backpropagation and optimisation algorithms are always employed together in the context of feedforward ANNs, this ensemble will hereafter be referred to as the *network training algorithm* in this article.

Although weight and bias variables are optimised based on the training data, choices still need to be made on which network training algorithm and loss function to use, on the number of hidden layers to include in the ANN architecture, on the number of neurons in each hidden layer, and on the specific activation function. Such parameters, which are not automatically optimised during training but need to be established beforehand, are known as hyperparameters. There exists a wide variety of strategies that can be employed for optimising hyperparameters of different types of ANNs for different problems. However, most of them naturally require a suitable number of data points in order to evaluate the performance of different hyperparameter configurations. These data points need to differ from those used for training the ANN in order to provide reliable estimates of the general predictive capabilities of the different models. Data used for this purpose are known as validation data. Since validation data are actually employed for improving the prediction model, they cannot also be used to evaluate the generalisation capability of the same model in an unbiased manner. For this reason, in the context of ANNs, available labelled data are typically sub-divided into three sets, commonly referred to as the training, validation and test datasets, with the latter only used to estimate the true general predictive capability of the final tuned model.

Proposed methodology

The basic underlying concept behind the proposed methodology for estimating the axial load in historical ties is fundamentally a simple one. It relies on using a suitable finite-element (FE) model to create a synthetic input-output dataset that is then processed and used to train feedforward ANNs. The trained ANNs can then be employed with dynamic characteristics extracted from experimentally-obtained vibration acquisitions to predict the axial load, as well as equivalent spring stiffnesses imposed at either end of the ties by actual boundary conditions. The steps involved in the proposed methodology are summarised in Fig. 3.

No specific experimental procedure is stated as part of the methodology since adaptability of required experimental inputs was in fact a motivating aim

behind its development. Instead, possible parameters that may be extracted from vibration acquisitions are presented along with the most relevant aspects that need to be taken into account when selecting the ones that will serve as inputs to the ANNs. Some key aspects that should be considered when designing the experimental procedure to obtain the selected inputs are also elaborated. Subsequently, the different steps that need to be followed to generate the required data for training and optimising the ANNs based on characteristics of the selected input parameters are elaborated. Finally, the process of optimising the hyperparameters of the feedforward ANNs until a suitable predictive performance is achieved is also described.

Data selection and experimental setup

Only two types of dynamic characteristics that may be extracted from vibration acquisitions are in fact useful for predicting the axial load sustained by a tie-rod: natural frequencies and components of the corresponding mode shape vectors. Being eigenvalues and eigenvectors, it is well-known that there are several values of these parameters that correspond to different natural modes of vibration of a structural system. If vibration acquisitions are obtained using contact sensors, it is typically most advantageous to place the accelerometers in positions where the mode shape amplitudes are greatest because the signal-to-noise ratio with respect to the natural mode of vibration will naturally be higher in these zones. One exception to this rule occurs when the mass of the accelerometer(s) is significant with respect to the distributed mass of the tie-rod. One advantage of using specifically developed ANNs for predicting the axial load in a tie-rod is that the position of accelerometers can be chosen in order to maximise the number of vibration modes that can be observed. This can contribute to improving the reliability of the predicted axial load since it adds redundancy in the estimation process. Additionally, if there are any specific accessibility issues or if a tie-rod contains significant discontinuities such as large connectors, the experimental procedure may be adapted accordingly.

As such, it is recommended to design the experimental procedure so that as many vibration modes as possible may be captured considering cost and accessibility limitations. Fundamentally, the natural frequency and shape vector of every vibration mode of a tie-rod
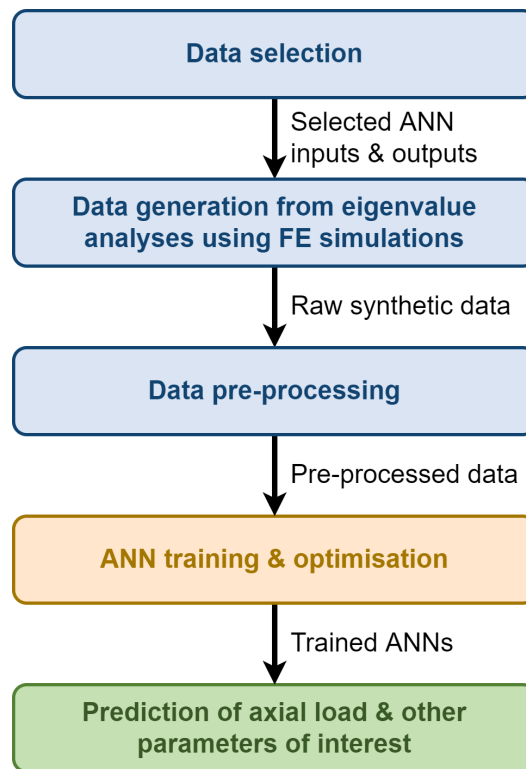
```
┌─────────────────────────────────────┐
│           Data selection            │
└─────────────────────────────────────┘
                    │ Selected ANN
                    ▼ inputs & outputs
┌─────────────────────────────────────┐
│    Data generation from eigenvalue   │
│      analyses using FE simulations   │
└─────────────────────────────────────┘
                    │ Raw synthetic data
                    ▼
┌─────────────────────────────────────┐
│          Data pre-processing         │
└─────────────────────────────────────┘
                    │ Pre-processed data
                    ▼
┌─────────────────────────────────────┐
│        ANN training & optimisation   │
└─────────────────────────────────────┘
                    │ Trained ANNs
                    ▼
┌─────────────────────────────────────┐
│      Prediction of axial load & other │
│        parameters of interest        │
└─────────────────────────────────────┘
```

Figure 3. Proposed methodology.

depends on its geometry, its loading and boundary conditions, and on the density and elastic properties of the material it is made of. Therefore, any data that can be gathered on the geometry of a tie or on its material properties will improve the reliability of the axial load estimate. Although all the previously proposed methods (Table 1) require accurate measurements of the tie-rod's geometry, none of them attempt to collect data on the elastic properties of the material despite the existence of fairly widespread non-destructive techniques that are able to do so. For the method proposed as part of this research, it is recommended to not only perform an accurate geometrical survey of the tie-rod being tested but also to use ultrasonic pulse velocity measurements to estimate the actual dynamic elastic modulus of the material it is made of. This allows for reduced uncertainty in the dataset to be generated using FE simulations (see subsection on data generation) and ultimately results in more reliable axial load estimates.

Although it is recommended to employ natural frequencies directly as inputs of the ANNs for predicting the axial load in a tie-rod using the proposed methodology, it is recommended to employ ratios between key components of each mode shape vector as predictors instead of the individual components themselves. This practice condenses the useful information provided by two mode shape components into a single input parameter, which simplifies the architecture of the ANNs and ultimately leads to a more computationally cost-effective solution.

Data generation

Once the dynamic characteristics that will be used to estimate the axial load have been selected, the data that will be used to train the ANNs must be generated using FE simulations. It is important to note that the dynamic characteristics that will serve as the input features of the feedforward ANNs (natural frequencies, ratios between mode shape components) will in fact be obtained from outputs of the FE simulations. Specifically, they will be obtained by performing eigenvalue analyses using the stiffness and mass matrices corresponding to different pre-defined initial configurations of the tie. Each example (or instance) constituting the dataset to be used for ANN training therefore corresponds to an FE simulation and the output features to be predicted by the ANNs are in fact specified as initial configurations of the simulations. Although these output features primarily refer to the axial load sustained by the tie and to the rotational stiffness of equivalent boundary springs, they may in theory also include any other relevant unknown parameter that is to be predicted by the ANNs. If a particular application requires

incorporating variations of other unknown parameters, such as the length of tie-rods for example, the range of variations that needs to be included in the training data will naturally depend on the specific needs of the application in question. It should be noted that specific guidance is given in this subsection only for applications which require treating the axial load and the stiffness of end constraints as unknowns. Nevertheless, the same philosophy used to generate the combinations of these parameters to be included in the synthetic dataset may be readily extended to other situations which may require treating other parameters as unknowns.

First, a base model must be created using the measured geometry of the tie-rod, including any connectors or changes in cross-section. Depending on the slenderness of the tie under investigation, Euler-Bernoulli or Timoshenko beam elements can be used for the base model. A linear elastic material model should be used with the elastic modulus set at the average value estimated using ultrasonic pulse velocity readings. Guidance on how to choose suitable transducers as well as the expression for relating the measured velocity of ultrasonic P-waves to the elastic modulus of an isotropic material can be found in many references [28]. Knowledge of the material density and the Poisson's ratio are required for computing the elastic modulus. The former can be assumed to be 7850 kg/m^3 or 7750 kg/m^3 depending on whether the tie is made of steel or wrought iron respectively. This information can typically be inferred from historical information on when the tie was installed. The Poisson's ratio can be assumed to be 0.3. The same assumptions for these two material parameters used for estimating the elastic modulus from the ultrasonic pulse velocity measurements should be employed for defining the material of the FE model. Additionally, if there are significant differences in the elastic moduli evaluated in different parts of a tie, this can be considered in the base model through the definition of different material models.

At first, three configurations of the base model with no axial load should be created in order to quantify the extreme boundary condition possibilities at both extremities of the tie's free span. Specifically, one model should be created with pin connections at both ends, one with fixed connections, and a third model with pin connections together with a rotational boundary spring at both ends (equivalent to the model shown in Fig. 1(a)). Based on the difference between the predicted frequency of the first vibration mode

from the models with pinned-pinned and fixed-fixed boundary conditions, the rotational stiffness of the boundary springs that effectively correspond to the fixed-fixed condition can be estimated through a simple parametric study. Specifically, the rotational stiffness corresponding to a fixed condition should be defined as the one for which the predicted frequency of the first vibration mode differs by less than 1% from that predicted by the model with the fixed-fixed boundary condition. Once this range has been determined, only the model with rotational springs needs to be used for generating the data for training the ANNs. It should be noted that the parametric study is not only useful for generating training data but also for interpreting eventual rotational spring stiffnesses that will be predicted by the ANNs.

The next step that needs to be performed involves establishing the maximum axial load that needs to be represented in the training data. In many cases, if a tie is accessible, observing the vibration response after a small impact can help to determine whether a tie is highly tensioned or very loose. In the latter case, the entire range of loads to be investigated may be limited to 30% of the axial load capacity of the tie assuming a reasonable yield strength for the material. In the former case, or if no such observation can be made, the full range of possible axial loads should be represented in the training data. Once the ranges of rotational spring stiffness and axial load that need to be represented in the training data have been determined, all the FE simulations that need to be run for generating a suitable dataset need to be defined. This can be achieved through the definition of four datasets that constitute different combinations of axial load and rotational spring stiffness: a main dataset, one with only pinned-pinned boundary conditions, one with only fixed-fixed boundary conditions, and one with additional training examples involving low axial loads. The main characteristics of these four datasets along with the recommended minimum number of examples in each are summarised in Table 2. Note that in the case of an apparently very loose tie, the reference maximum value to which the prescribed ranges for subsets shown in Table 2 refer to corresponds to the aforementioned 30% of the estimated axial load capacity of the tie.

The axial load variations in each of the subsets of the main dataset (low, mid-range and high axial loads) can be simply defined using a linearly spaced vector between the minimum and maximum values of the

Table 2. Recommended minimum number of input-output examples to include in generated dataset.

Dataset	Axial load range (% of max. value)	Number of variations		
		Axial load	**Boundary conditions**	**Total**
Main dataset: low axial loads	*1% < N ⩽ 10%*	*3*	*250**	*1050*
Main dataset: mid-range	*10% < N ⩽ 50%*	*3*	*+*	*1050*
Main dataset: high axial loads	*50% < N ⩽ 100%*	*2*	*$2 \times 50^{\dagger}$*	*700*
Main dataset - Total	*1% < N ⩽ 100%*	*8*		*2800*
Pinned boundary conditions	0% < N ⩽ 100%	500	1	500
Fixed boundary conditions	0% < N ⩽ 100%	500	1	500
Extra low axial load dataset	0% < N ⩽ 1%	8	200* + $2 \times 50^{\dagger}$	2400
Synthetic data - Total				**6200**

* Symmetric boundary condition variations in which the magnitude of both left and right spring stiffnesses are varied but are always kept equal to each other.

† Two asymmetric sets of at least 50 boundary condition variations. In the first asymmetric set, the spring stiffness corresponding to the left end is kept constant while that corresponding to the right end is varied. In the second asymmetric set, only the spring stiffness corresponding to the left end is varied.

ranges shown in Table 2 as a function of the previously established maximum axial load value that needs to be represented in the training data. As shown in Table 2, at least 350 different boundary condition variations should be defined for the main dataset to be combined with at least 8 axial load variations, resulting in a minimum of 2800 training examples in that dataset. The boundary condition variations can also be defined using linearly spaced vectors of equivalent rotational spring stiffnesses spanning from 0 kNm/° up to a value which is twice as much as the previously estimated rotational spring stiffness corresponding to the fixed condition. If the minimum number of asymmetric boundary condition variations shown in Table 2 is chosen, a linearly spaced vector of 50 elements should first be defined. Then, one set of boundary condition variations should be defined by assigning that vector to the rotational spring at the right end of the tie while the value for the rotational spring at the left end is kept constant for all combinations at the maximum value to be included in the dataset. Similarly, the next set of asymmetric boundary condition variations would then involve assigning the linearly spaced vector of 50 elements to the left spring while keeping the value of the right spring constant at the same maximum value. The set of symmetric boundary condition variations can simply be defined by assigning a linearly spaced vector of equivalent rotational spring stiffnesses to both the left and right ends.

As its name suggests, the rotational stiffness at both ends of all combinations in the pinned boundary conditions dataset should be set to zero, while the

axial load is varied using a linearly spaced vector of at least 500 elements from zero to the maximum value in the previously established range. Similarly, the fixed boundary condition dataset should consist of the same vector of axial loads but with the rotational stiffnesses at both ends set at the previously estimated rotational spring stiffness corresponding to the fixed condition. The final dataset required for generating suitable synthetic data should be made up of at least 2400 examples with low axial loads and similar boundary condition variations as those defined for the main dataset. The minimum number of variations specified in Table 2 can also be defined by generating linearly spaced vectors. This last dataset has been specified because previous research reveals that it is more difficult to obtain accurate solutions to this particular inverse vibration problem at low levels of axial load [8,13,21]. This can in part be attributed to the fact that measurable dynamic characteristics of a tie become less sensitive to changes in boundary conditions as the axial load it sustains increases.

Once all the configurations of FE simulations (or output features of the synthetic data) have been defined, they should be collected in tabular form and any duplicates should be eliminated. The input features of the synthetic data can then simply be obtained by performing an eigenvalue analysis for each pre-defined configuration of the FE model and by collecting the relevant predicted dynamic characteristics in tabular form. In order to achieve this, it is most convenient to define a batch analysis job which can be relatively straightforward to program nowadays

for many commercial FE packages. For the case study presented in this article, all numerical analyses were performed using the DIANA FEA commercial package[29] and a similar procedure as that used by Saloustros et al. for the probabilistic assessment of seismic vulnerability[30] was employed for defining the batch analysis job. It should be noted that FE eigenvalue analysis performed using beam elements is not very computationally expensive and results for a single training example can typically be obtained in a matter of seconds on most modern personal computers. This means that the generation of all the necessary data required for ANN training and optimisation is likely to require less than a day of computation on most personal computers.

Data pre-processing

Once the results from FE simulations have been collected and manipulated to form a synthetic dataset, two important pre-processing steps need to be performed before ANN training: feature scaling and noise addition. As previously described, the synthetic data will consist of natural frequencies and ratios between mode shape components as inputs and axial loads, equivalent rotational spring stiffnesses, and any other relevant unknown parameter to be predicted by the ANNs as outputs. Each of these variables represent fundamentally different quantities whose range of possible values can differ drastically. This means that any functions expressing relationships between them are likely to be characterised by very steep gradients in very localised zones which is likely to make the process of learning through any network training algorithm highly inefficient or even impossible. In order to address this issue, all the variables present in the synthetic data should be transformed to a normalised scale. There exist different possible ways of performing such transformations and their effectiveness typically depends on the characteristics of the variables and of the activation functions employed in different layers of feedforward ANNs. For the hyperparameters recommended as part of the methodology proposed in this article, it was found that applying a feature scaling method commonly referred to as min-max scaling results in adequate performance. Specifically, this involves transforming all the examples of each input and output variable to a range of [0,1] using the expression shown in Eq. (1).

$$x' = \frac{x - min(x)}{max(x) - min(x)} \qquad (1)$$

Where x refers to the original value of an element of an input or output variable, while x' corresponds to the transformed value. Naturally, to be able to interpret resulting outputs predicted by the ANNs, they need to be transformed back to their original scale using the inverse of the function shown in Eq. (1).

In addition to feature scaling, it is also important to add noise to each vector of dynamic characteristics acting as an input variable before training the ANNs. This pre-processing step is very important to ensure that the ANNs perform well when employed with real-world data. Trials performed as part of this research revealed that when an ANN has learnt only from training data generated by simulations, it can show extremely good prediction performance across the entire range of interest when tested with different data generated from simulations, but still perform poorly when fed with dynamic characteristics extracted from vibration acquisitions. This is because real world data can be influenced by many factors, including background noise during vibration acquisitions, which can lead to small deviations when compared to dynamic characteristics predicted by numerical simulations. If such variations are not included in the training data, the resulting ANN will inevitably not be well equipped to deal with them.

As such, a Gaussian white noise profile with a specific standard deviation should be superimposed to the elements of each input variable in the synthetic data. Specifying an adequate standard deviation for each input variable requires appropriate consideration of the type of quantity it represents, the possible errors that can occur during the measurement of this quantity, and the range of values present in the synthetic data sample. For the purpose of estimating the axial load in tie-rods, some heuristics are proposed as part of this research for the addition of the noise profiles. For input variables consisting of ratios between mode shape components, the standard deviation of the Gaussian white noise can be set at 0.5% of the range present in the synthetic data. For each frequency used as an input variable, the standard deviation of the generated noise profile should always be greater than the theoretical frequency resolution of the modal analysis that will be performed for its estimation. Naturally, this value does not consider environmental and operational conditions

that can add significant uncertainty to the measurement of natural frequencies. As such, the specified standard deviation of the Gaussian noise profile typically needs to be greater than this theoretical frequency resolution. For frequencies that will be based on simultaneous vibration acquisitions taken at 2 or more locations excluding any placed in the vicinity of a vibration node (location with zero mode shape amplitude), the standard deviation of the noise profile can be set as the minimum between 0.1 Hz and 2% of the range represented in the synthetic data. For natural frequencies that will be estimated using a single vibration acquisition excluding vibration node locations, the standard deviation of the noise profile can be set as the minimum between 0.25 Hz and 5% of the range represented in the synthetic data. Of course, if the noise is to be added to the synthetic data after feature scaling, the standard deviations estimated from the aforementioned heuristics should be transformed before superposition in exactly the same manner as the elements of the corresponding input variable using Eq. (1).

ANN training and optimisation

Once all the synthetic data have been pre-processed, they only need to be separated into training, validation, and test subsets (see section on ANNs) before proceeding to ANN training and optimisation. The data to be allocated to each subset should be randomly selected from the ranges of values present in the entire synthetic dataset. For the purpose of estimating the axial force in tie-rods using the methodology proposed in this article, 70% of the data should be allocated to the training subset, 20% to the validation subset, and 10% to the test subset. This will ensure there are sufficient examples in each subset to obtain suitably performing feedforward ANNs.

As part of the proposed methodology, only two ANN hyperparameters need to be optimised: the number of neurons to include in the first and second hidden layers of a feedforward ANN. A suitable predictive performance can be achieved without changing any other hyperparameter. Specifically, a feedforward ANN architecture consisting of 2 hidden layers should be used. For all neurons in these two layers, a hyperbolic tangent transfer function should be used as activation function[31], while a simple linear transfer function should be used for activation in the output layer. The backpropagation learning algorithm should be used together with Levenberg-Marquardt optimisation for

updating weights and biases during network training[32] and the mean squared of errors should be used as the loss function to be minimised. For stopping the iterative optimisation algorithm, 20% of the elements of the training dataset should be randomly selected and allocated to an "Early stopping" dataset. This subset of the training data should not be directly considered by the network training algorithm for optimising weights and biases, but the iterative algorithm should be stopped when the network performance on this subset fails to improve or remains the same for 50 epochs in a row. This occurrence would be a clear sign of *overfitting*, whereby although the network's capability to represent relationships in data used for learning is improving, its ability to generalise to new unseen data is worsening. In this case, as shown in Fig. 4, the configuration with the lowest error on the Early stopping dataset before this occurrence should be selected to prevent overfitting. If this condition still has not been met after at least 1000 epochs, network training may also be stopped and the configuration corresponding to the best performance on the Early stopping dataset should be selected. It is important to note that these recommended epoch thresholds may have to be modified if the synthetic dataset employed contains much more elements compared to the minimum recommended as part of the proposed methodology.

As previously mentioned, the number of neurons to use in the first and second layers of the feedforward ANNs are still left to define. A *grid search* technique[22] can be used for the selection of these two hyperparameters. This technique systematically searches through a grid of possible hyperparameter configurations. In this case, possible hyperparameters now simply refer to possible numbers of neurons in each hidden layer and the search seeks to find the configuration resulting in the smallest mean prediction error over all outputs in the validation data. First, a grid search should be made using only ANNs with a single hidden layer, varying the possible number of neurons in this layer from 5 to 100. At least the 3 best performing configurations for the first hidden layer should be retained. Then, a second grid search should be performed over ANNs with two hidden layers, but limiting the possible options for the first layer to those retained after the first grid search. For this second grid search, the possible options to be considered for the number of neurons in the second layer may be limited to 5 equally spaced numbers that are smaller than
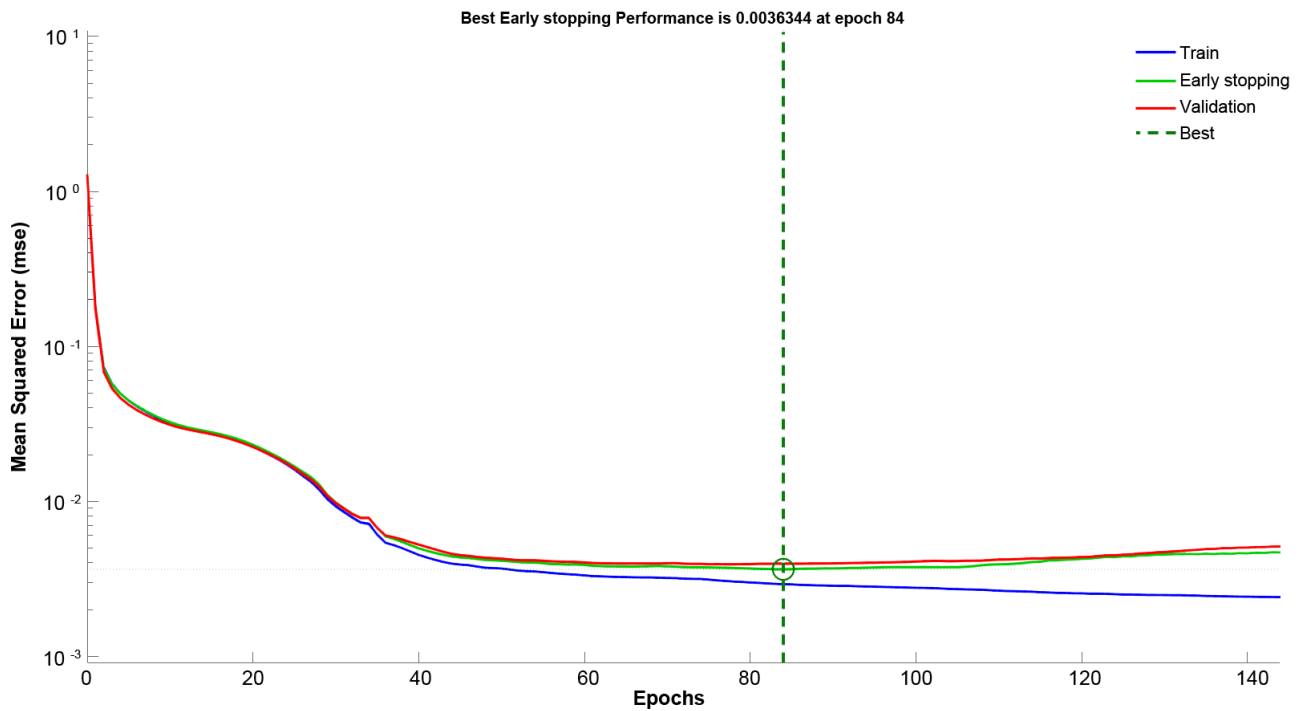
Figure 4. Example evolution of mean squared error in different datasets during ANN training.

Application to case study

the selected best performing options for the first layer. This means that the second grid search will consist in evaluating at least 15 different possible configurations. At this point, it is worth reiterating the fact that weights and biases are optimised on the basis of a randomly selected subset of the synthetic data and that they would differ slightly if another random selection was made. Therefore, it is possible to achieve improved performance by training multiple ANNs on different random selections (of the same size) from the synthetic data and keeping the average of the multiple predicted outputs. For this reason, it is recommended to train 3 ANNs for each network configuration evaluated during the grid search procedure, and to train 10 ANNs of the final chosen configuration to be used for predictions. It should be noted that the entire recommended grid search procedure as well as the training of the final 10 ANNs to be used for prediction can be performed in less than a day using a personal computer if the minimum recommended number of data samples are used. Naturally, the required computation time will increase if larger datasets are used. Once the final ANNs have been trained, they may be used to obtain instantaneous predictions of the axial load and other outputs based on experimentally obtained dynamic characteristics.

The ties that are the subject of the chosen case study are shown in Fig. 5. They are found at a height of approximately 14.3 m just below the lantern tower (*cimborio*) in the main crossing of the church of the monastery of Sant Cugat, an important medieval heritage structure near Barcelona consisting of different parts built mostly between the mid-12th century and the 15th century. The ties were installed as part of strengthening and repair works which were performed towards the end of the 19th century due to concerns over the outward leaning of elements such as the bell tower and visible cracks in several elements including the *cimborio*[33]. Recent results from a monitoring campaign reveal that one of the pillars supporting the *cimborio* is still experiencing an active outward rotation[34]. Since ties are meant to contribute to resisting the lateral thrust exerted on the pillar, knowledge of the actual force resisted by the ties can definitely contribute to a better understanding of the actual loading conditions.

Vibration testing and modal analysis

Both ties forming part of this study consist of three segments unified by the connectors that join them. Several geometrical measurements of both ties were made. The disposition along the length as well as the cross-sectional dimensions of both ties were found to be almost identical (characterised by coefficients
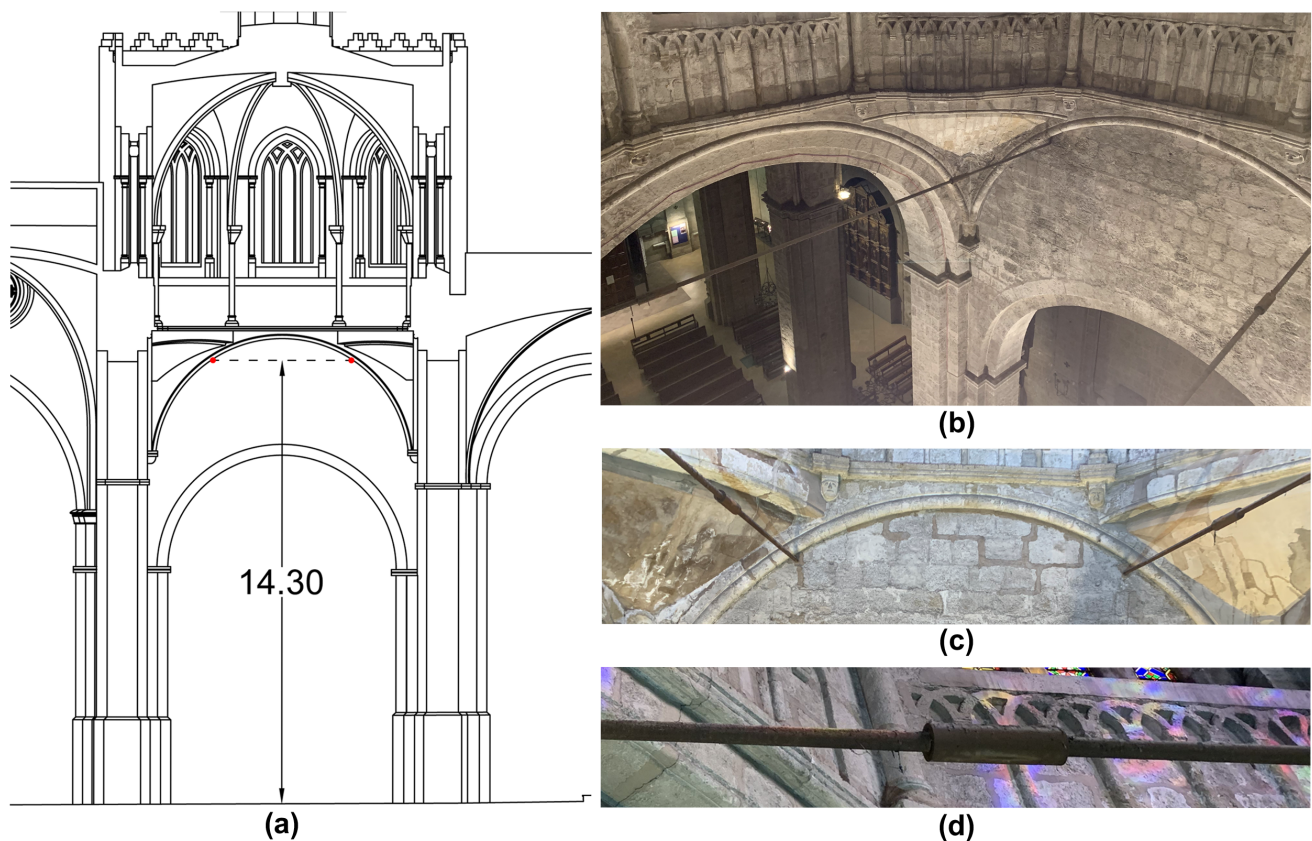
Figure 5. (a) Location of the ties shown in a longitudinal cross-section of the church going through the crossing (all dimensions in m). (b) Picture of the ties from above showing the connection of the western tie to the wall on the northern side. (c) Connection of both ties to the wall on the southern side. (d) Close-up view of a connector.

of variation of less than 1%), with the average measured dimensions shown in Fig. 6(a). This means that a FE model with a unique geometry can be used for simulating the behaviour of both ties. As described in the proposed methodology (subsection on data selection and experimental setup), ultrasonic pulse velocity measurements were also made using a PROCEQ Pundit PL-200[35] commercial ultrasonic testing instrument equipped with 500 kHz transducers. From these measurements, the elastic modulus of the material making up both ties was estimated as being 174 GPa.

The main components of the data acquisition system employed for the vibration tests include an instrumented impact hammer (PCB 086C03), piezoelectric accelerometers, and an embedded real-time controller (cRIO-9064) equipped with vibration input modules (NI-9234). Some of these components are shown in Fig. 6. Specifically, vibration signatures recorded with a sampling frequency of 5 kHz from a total of three uniaxial accelerometers were used for modal analysis. The exact locations of these accelerometers for the tests on each tie are shown in Fig. 6(a). These locations were chosen so as to identify as many modes

as possible considering the available equipment and time for testing. As shown, the western tie was only instrumented with 2 accelerometers. This modification had to be implemented on the day of testing due to time constraints. In addition to ambient vibration tests which simply involve recording the vibration signatures of the ties with no specific excitation, tests which involve exciting the tie at specific locations using the instrumented hammer were also performed. A total of 11 vibration acquisitions were recorded while testing the eastern tie and a total of 7 were recorded for the western one. The average duration of impact hammer tests was of 2.4 min while that of ambient vibration tests was of 7.4 min.

Modal analysis was performed using the Frequency Domain Decomposition (FDD) technique[36], which relies on selecting clearly distinguishable peaks from singular values of the power spectral density matrix or frequency response function as shown in Fig. 7(b). The MACEC toolbox[37] for MATLAB[38] was used for performing these computations.

As summarised in Table 3, a total of 4 modes could be identified from the acceleration records. Although vibration modes could clearly be identified, it is worth
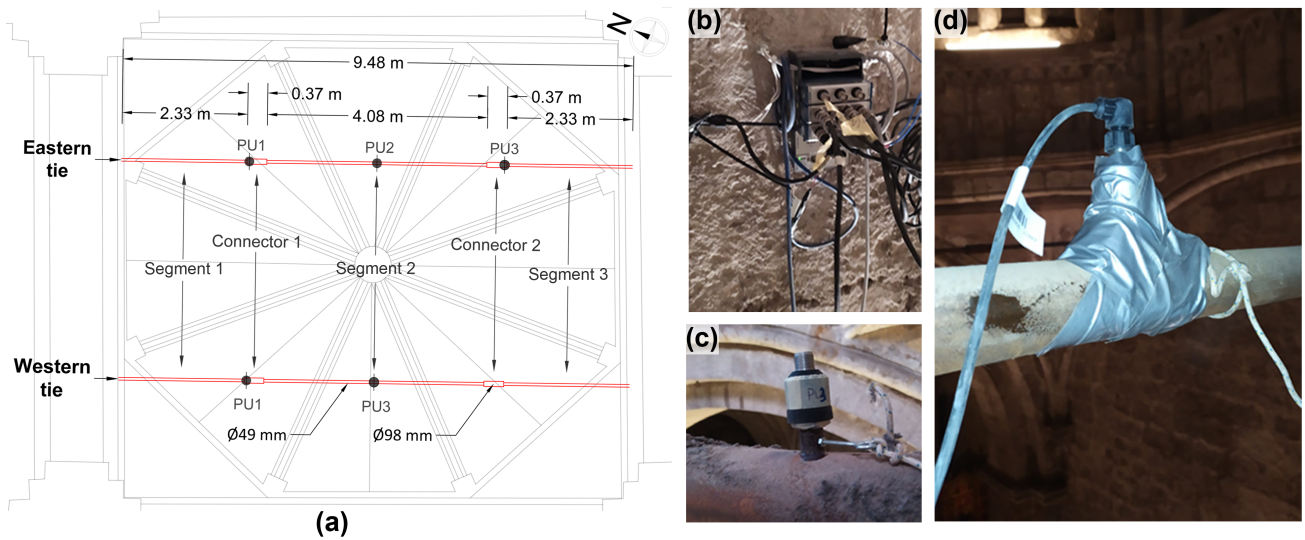
Figure 6. (a) Average measured dimensions and locations at which accelerometers (PU1, PU2 and PU3) were placed. (b) Real-time controller fixed on the northern wall next to the eastern tie. (c) Uniaxial accelerometer before connecting wires. (d) Accelerometer PU3 placed on the western tie.
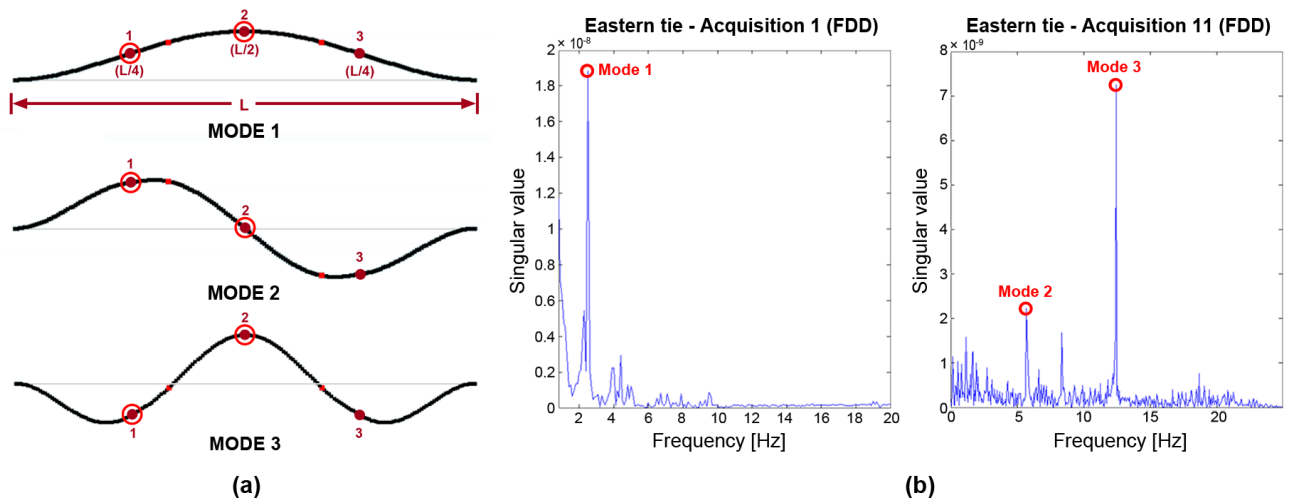

Figure 7. (a) First three expected resonance mode shapes predicted by numerical model of fully clamped tie. Records from accelerometers placed at the locations shown by points 1 to 3 on the eastern tie were used for modal analysis. On the western tie, accelerometers were only placed at locations 1 and 2. (b) Examples of natural frequencies identified using the Frequency Domain Decomposition (FDD) technique.

mentioning that the acquired acceleration records were characterised by a relatively high level of noise. The use of an excessively high sampling frequency during testing could most definitely have contributed to this situation.

ANN training and results

In order to be able to use the same ANNs for predicting the axial load in the eastern and western tie, only mode shape components from locations 1 and 2 shown in Fig. 7(a) were used for defining input variables. Given the location of accelerometers with respect to vibration nodes (see Fig. 7(a)), this means that adequate mode shape ratios could only be defined for modes of odd index (modes 1 and 3). As such, only the 6 quantities shown in Table 3 were chosen as input variables for

prediction. Since both the geometric properties and elastic modulus were determined accurately as part of the experimental procedure, only the axial load and equivalent rotational spring stiffnesses at both ends of each tie were defined as outputs to be predicted by the ANNs.

A synthetic dataset consisting of 8730 input-output examples was generated from FE simulations using the procedure described as part of the proposed methodology (see subsection on data generation and Table 2). The parametric study forming part of this procedure revealed that a rotational spring stiffness of approximately 43.6 kNm/° corresponds to a fixed condition (see Fig. 8). As previously described, the maximum rotational spring stiffness included in the

Table 3. Dynamic parameters estimated from vibration acquisitions using the FDD technique. The mode shape ratio values refer to the amplitude measured at location 2 divided by that measured at location 1 (see Fig. 7(a)).

Tie	Natural frequency [Hz]				Mode shape ratio (loc. 2/loc. 1)	
	Mode 1	Mode 2	Mode 3	Mode 4	Mode 1	Mode 3
Eastern tie	2.55	6.00	12.44	21.42	1.75	-1.60
Western tie	2.17	5.05	11.46	20.10	1.8	-1.55

entire synthetic dataset thus consisted of twice this value. In summary, the synthetic dataset generated for this case according to the proposed methodology contained axial loads that varied from 0 kN to 200 kN and rotational spring stiffnesses that varied from 0 kNm/° to 87.2 kNm/°. The specific combinations of axial loads with symmetric and asymmetric boundary conditions included in the synthetic dataset are shown in Fig. 9. It should be noted that the data points shown in the figure have been grouped according to the four datasets defined in the subsection of the proposed methodology on data generation (see Table 2). The distributions of the aforementioned 6 input variables collected after performing the FE simulations are shown in Fig. 10.

Based on the heuristics presented in the subsection of the proposed methodology on data pre-processing, a Gaussian white noise profile with a standard deviation of 0.1 Hz was superimposed to the input vectors corresponding to the first and third natural frequencies while one with a standard deviation of 0.25 Hz was added to the input vectors corresponding to the second and fourth natural frequencies. The standard deviation of the noise profiles used for the input vectors with mode shape ratios from the first and third modes were defined as 0.003 and 0.004 respectively using the same set of heuristics. Following the grid search procedure described in the subsection of the proposed methodology on ANN training and optimisation, the final ANN architecture to be used for prediction could be defined. It consisted of 2 hidden layers, the first with 34 neurons and the second with 10. As described in the proposed methodology, 10 such ANNs were trained so that the average of their outputs could be used for predictions.

Evaluating the performance of these 10 ANNs over the 873 elements of the test dataset reveal an average root-mean-square error ($\text{RMSE}_{\text{Test}}$) of 0.28 kN for axial load predictions, 0.73 kNm/° for predictions of the rotational spring stiffness on the left end, and 1.16 kNm/° for predictions of the rotational spring stiffness on the right end. Regression plots for the three outputs over the validation and test datasets are also shown in Fig.

11. As can be seen, prediction errors from the final ANNs are very small, particularly considering the range of values being tested and the fact that none of the reviewed analytical model-based methods (see Table 1) can be directly applied to this particular case due to the presence of two connectors on each tie. For instance, FE simulations can be used to show that direct application of two such analytical model-based methods[8,13] to this case would result in prediction errors that are greater than 50% of the actual axial load. Some discrepancies in the ANN predictions can be observed from Fig. 11, most notably related to the prediction of the equivalent rotational spring stiffnesses at either end of the tie-rod. However, the greatest differences always occur for simulated stiffness values equal to 0 kNm/°, an ideal pinned condition that is unlikely to be encountered in most practical applications. Nevertheless, even in these cases, the sparsity of outliers and the low $\text{RMSE}_{\text{Test}}$ values suggest that the average prediction from 10 ANNs will undoubtedly still be sufficiently accurate to provide a good understanding of the boundary conditions. Based on these comparisons with FE simulation results, it is clear that the achievable accuracy of the proposed method employing ANNs for predicting the axial load in historical ties is more than satisfactory for most practical applications.

After the 6 dynamic characteristics extracted from vibration tests on the two ties were fed into the trained ANNs (see Table 3), the average predicted axial load was found to be 15.76 kN for the eastern tie and 1.03 kN for the western one. Both these values can in fact be considered as being low and suggest that the ties are currently not contributing significantly to resisting lateral thrusts imposed by the geometry of the masonry structure. This may partly be due to the specific height and location at which they are placed, which can be considered as being rather inefficient with respect to the structural form and expected load paths in the masonry structure. Furthermore, these results concur with observations made during testing indicating that the vibration response of both ties is characterised by a relatively loose behaviour.
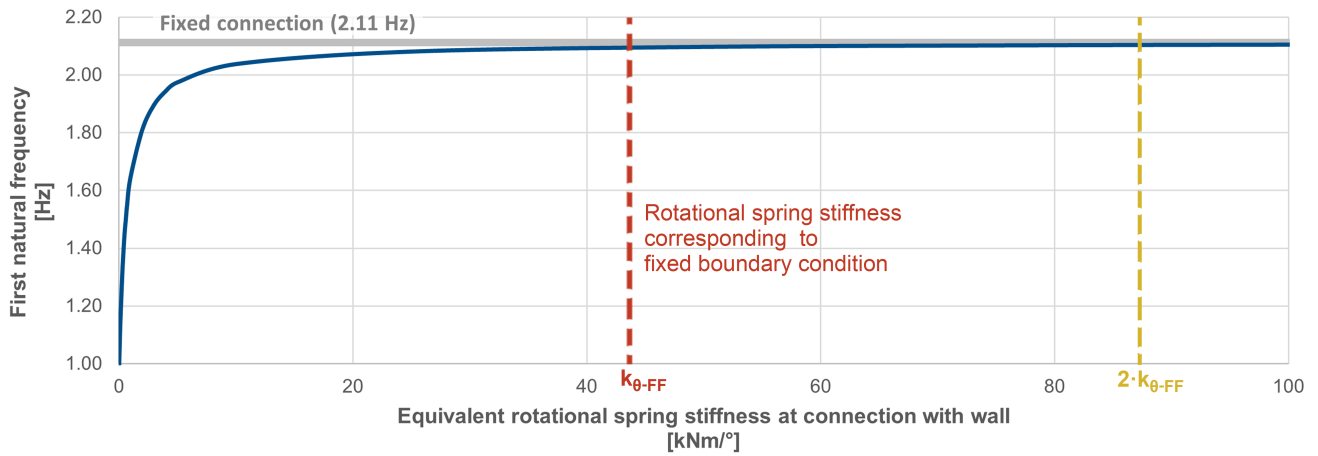
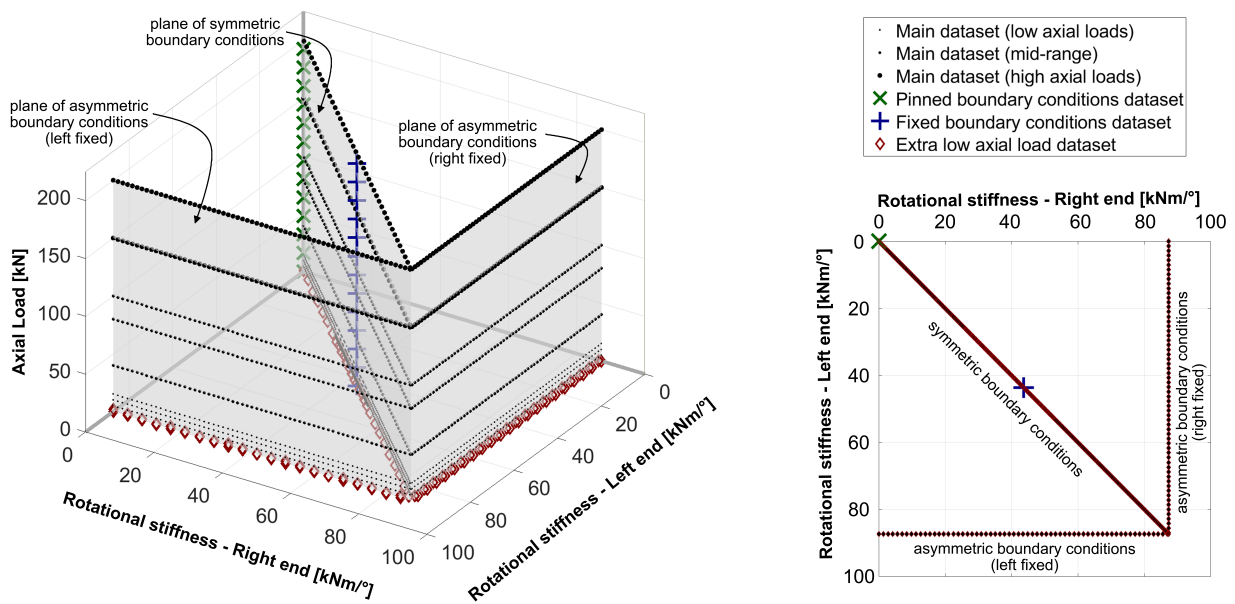**Figure 8.** Effect of rotational stiffness at the extremities of the free span of a tie-rod.

Figure 9. Combinations of axial load and rotational spring stiffnesses used to generate synthetic data.
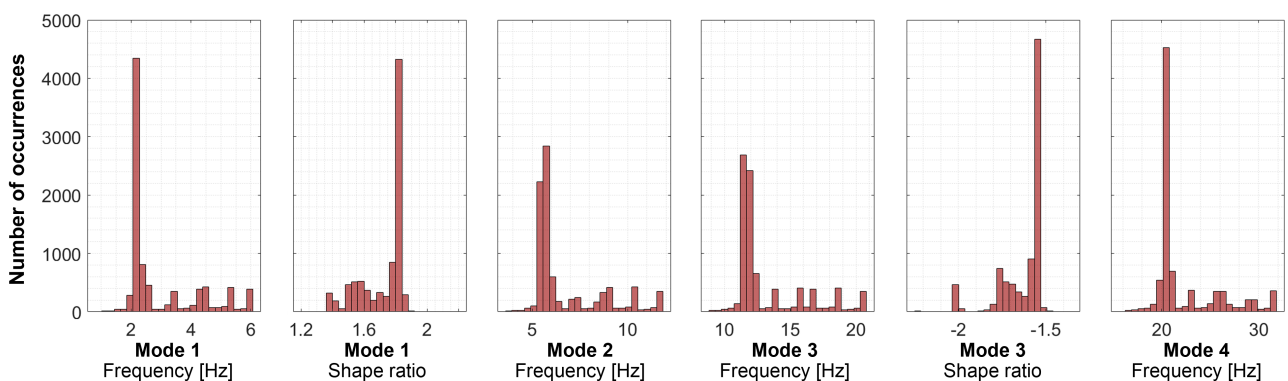

Figure 10. Histograms showing the distribution of input data used for training and testing the ANNs.

With respect to boundary conditions, as previously mentioned, a parametric study revealed that a rotational stiffness of 43.6 kNm/° clearly corresponds to the fixed-fixed condition for this case (Fig. 8). The predicted equivalent rotational spring stiffnesses at the left and right end of the ties turned out to be 49 kNm/° and 26 kNm/° respectively for the eastern tie. For the western tie, the same spring stiffnesses turned out to be 22 kNm/° and 26 kNm/° respectively. By analysing the results of the parametric study shown in Fig. 8, it can be said that all of the predicted rotational spring stiffnesses for both ties correspond to a boundary condition whose
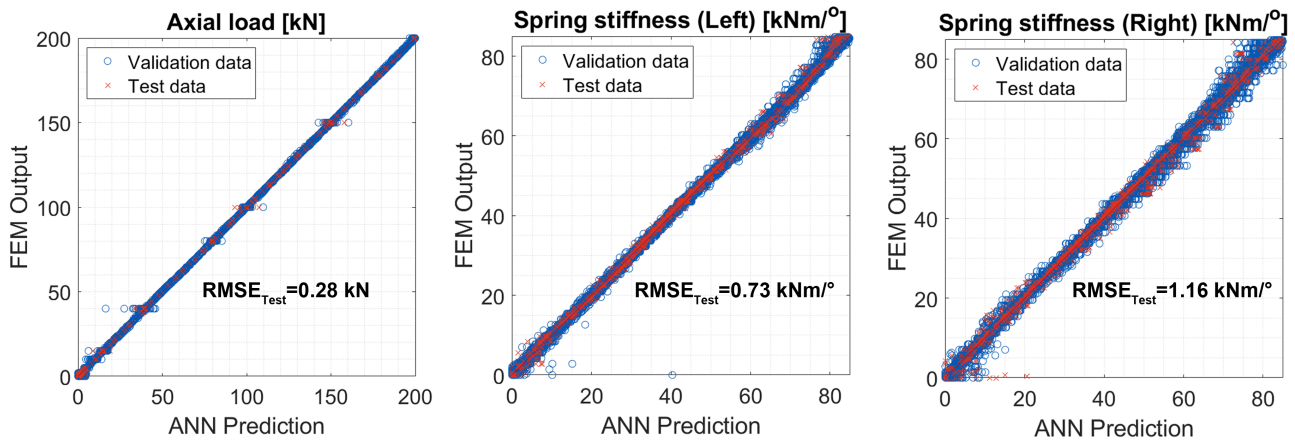
Figure 11. Regression plots showing the relationship between theoretical values computed using FE models and predictions from ANNs for the test and validation data. The individual data points from these datasets for all 10 trained ANNs are plotted. The average root-mean-square error computed over the test dataset (RMSE$_{Test}$) for each ANN is also shown.

Table 4. Comparison between natural frequencies predicted by calibrated numerical models and those estimated from the vibration tests.

| | Tie | Natural frequency estimate [Hz] | | Relative change from FE estimate |
		FE model (configured from ANN results)	Vibration acquisitions	
Mode 1	**East**	2.71	2.55	6.11%
	West	2.16	2.17	0.79%
Mode 2	**East**	6.32	6.00	5.22%
	West	5.63	5.05	10.82%
Mode 3	**East**	12.63	12.44	1.57%
	West	11.74	11.46	2.42%
Mode 4	**East**	21.56	21.42	0.66%
	West	20.48	20.10	1.89%

behaviour is very close to that of a fixed connection. This prediction is in good agreement with the fact that no gaps could be observed around the ends of the ties where they go through the wall (see Fig. 5(c)). In fact, it appears that the stiffness of these connections has been ensured by filling the area at the interfaces between the walls and ties with a cement mortar.

In order to further validate the proposed methodology, the axial load and rotational spring stiffnesses of the eastern and western tie predicted by the ANNs were used to configure a FE model of each tie. The first four natural frequencies obtained by performing an eigenvalue analysis using these models are compared in Table 4 to the first four natural frequencies obtained experimentally through vibration tests. In general, we can see that there is a good agreement between the experimentally determined natural frequencies and those predicted by the calibrated models. This indicates that the models provide a good representation of reality and that the tensile loads can be considered as being reliable.

A greater relative difference can be identified in Table 4 between frequency estimates of the second mode of vibration, particularly in the case of the western tie. This can most likely in part be attributed to the fact that the second mode shape is known to contain a node exactly at the midspan for symmetric boundary conditions. The low vibration amplitude around this location can therefore significantly hinder the ability of the accelerometer placed there to register this mode of vibration. In the case of the western tie, this means that the estimated frequency mostly relies on the records from a single accelerometer. In fact, a greater relative difference can be observed for the natural frequencies of the western tie across three of the four identified modes of vibration. This may be attributed to the fact that one less sensor was used for the tests on this tie. Despite the existence of these specific disparities between the simulated and experimentally determined structural behaviour, the good general agreement is a clear indication that the proposed methodology is robust.

Relative importance of ANN inputs

Although ANNs have received considerable attention across a wide range of scientific fields due to the superior predictive power they have often been able to demonstrate compared to traditional approaches, they have also received significant criticism regarding the lack of explanatory insight they provide. As a consequence, there have been considerable research efforts on methods aiming to provide explanatory insight into the relative influence of variables used as inputs to ANNs for prediction. According to a study performed by Olden et al.[39], which compares nine different methods for assessing variable contributions in ANNs, one of the most accurate methods for achieving this purpose is known as the *connection weight approach*[40]. The method involves computing the product of all raw input-hidden and hidden-output weights connecting each input neuron and output neuron and summing these products across all hidden neurons[39]. As a result, an importance score is obtained for each input with respect to each output that is predicted by the ANN. Although this value can be used to rank inputs according to their relative importance for predictions made by a single ANN, it is important to note that it cannot be compared across several ANNs. This is because different ANNs may be characterised by weights whose magnitude can differ significantly, even if trained for the same purpose. Since the importance score is computed on the basis of raw connection weights, its value is only meaningful within the context of other weights in the same ANN. Nevertheless, the rank of each input with respect to its relative importance for predicting a particular output can naturally be compared across different ANNs. Since the average output from 10 ANNs is used for prediction as part of the proposed methodology, the average rank evaluated using the connection weight approach across all these ANNs was employed to assess the relative importance of each input feature. The average rank of each input with respect to the prediction of each output for the ANNs used as part of the presented case study is shown in Fig. 12. Error bars are used to show the full range of ranks determined for each input. For each output, the input feature with the highest average rank has been coloured in green while that with the lowest average rank has been coloured in red.

The first observation that can be made from the estimated ranks is that the relative importance of most of the selected input features tend to be well balanced. The error bars shown in Fig. 12 reveal that there are considerable fluctuations in the rankings across the 10 trained ANNs with many of the input features occupying ranks that vary between the 2nd and 5th position in terms of relative importance for prediction. This demonstrates that the chosen input features do indeed provide useful information for estimating axial loads and constraint stiffness, and highlights the importance of using the average value of predictions from multiple ANNs to ensure robust prediction performance.

Nevertheless, it does appear that the second natural frequency is consistently ranked amongst the least important input features for prediction of all three outputs. Given the location of antinodes in the shape of this vibration mode, it is likely to be one of the modes most influenced by the lumped masses of the connectors. This could make the frequency of this vibration mode less sensitive to changes of the axial load and constraint stiffness, which would explain why it appears to play a less important role in predictions. Finally, it is interesting to note that the third mode of vibration is consistently ranked amongst the most important predictors for determining the axial load and that the fourth mode of vibration appears to be relatively important for prediction of constraint stiffness.

Conclusions

This research has proposed a novel methodology employing Artificial Neural Networks (ANNs) for the estimation of the axial force in historical ties from outcomes of vibration tests. Although this particular inverse vibration problem has received considerable research interest in the past, many of the most popular analytical model-based methods cannot be applied to cases where ties contain significant discontinuities or irregularities. In addition to being applicable to such cases, the proposed methodology relies on an experimental procedure that can be adapted to specific constraints of a particular case and the methodology itself may be adapted to best utilise useful experimental results for predictions. In fact, the proposed methodology stands out from all reviewed existing methods for solving this problem as being the only one that displays all three of the aforementioned characteristics.

A validation of the proposed methodology is presented involving its application for the estimation of
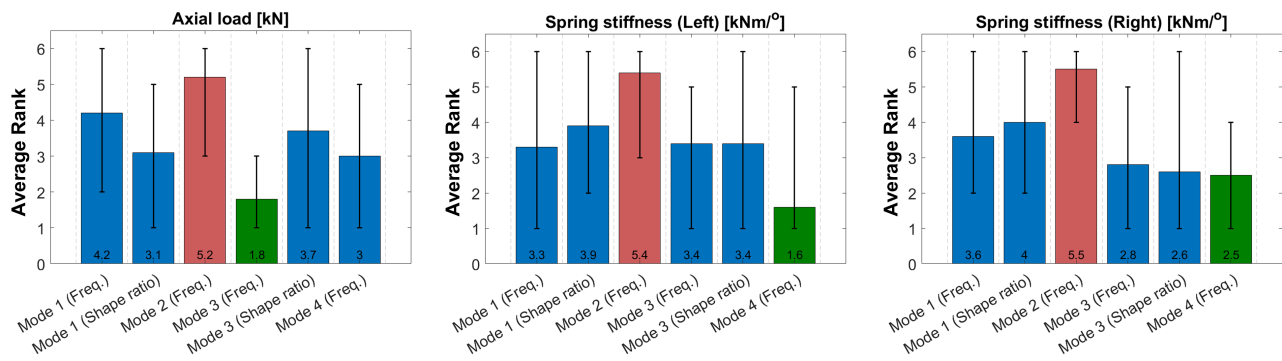
Figure 12. Average rank for each input feature with respect to each output that can be predicted by the ANNs. The full range of ranks determined for each input over the 10 ANNs is also shown with error bars. Note that greater bar heights indicate a lower rank.

the axial load in two tie-rods found in an important heritage structure in Catalonia. Both ties consist of three segments joined together by two larger connectors and it was estimated that they sustain relatively low axial loads (15.76 kN and 1.03 kN). Although previous research shows that the latter condition can significantly hinder the ability of obtaining accurate solutions for this inverse vibration problem[8,13,21], coherent predictions on the stiffness of the connections to masonry walls could also be made in addition to the axial load predictions. This outcome combined with the very small differences observed over the complete range of possible output values between Finite Element (FE) results and the ANN predictions from applying the methodology are clear indicators of its robustness.

It must be said that there exist nowadays a multitude of different Machine Learning (ML) algorithms that have found useful applications in a truly diverse range of fields. As such, there most definitely exist certain types of ML algorithms, including different ANN architectures, that can prove to be more efficient than the proposed feedforward ANN at solving this particular inverse vibration problem. However, the proposed methodology is clearly able to produce sufficiently accurate results for many practical purposes. In this case, a suitable performance level is attained in large part thanks to the incorporation of domain knowledge when designing the synthetic data to be used for ANN training. Such approaches have in fact recently been identified by leading Artificial Intelligence (AI) practitioners as being crucial for improving the performance of AI solutions in real-world applications[41].

Nevertheless, it is important to highlight that the presented validation case study required only axial loads and constraint stiffnesses to be assumed as unknowns. In practice, certain applications may require additional geometrical or material parameters to also be considered as unknowns. This may include situations involving ties that have suffered from significant damage or deterioration. Although the same philosophy used as part of this research to generate combinations of features for training ANNs may in principle be extended to consider other unknowns, more application cases are required to develop specific guidance and fully demonstrate the validity of the proposed methodology for such situations. In fact, an extension of the presented research could involve a specifically designed experimental campaign to explore a greater range of variations and to evaluate the effect of different acquisition conditions on predictive performance. This could contribute greatly to improving the proposed methodology.

Finally, the versatility of the new proposed methodology employing ANNs indicates that it may be easily adapted to be combined with other novel approaches for estimating the axial load in historical ties, e.g. to improve the accuracy of predictions derived from measurements obtained using contactless techniques.

Acknowledgements

Funding

Declaration of conflicting interests

The Authors declare that there is no conflict of interest.

References

1. Camassa D, Castellano A, Fraddosio A et al. Dynamic Identification of Tensile Force in Tie-Rods by Interferometric Radar Measurements. *Applied Sciences* 2021; 11(8): 3687. DOI:10.3390/app11083687.

2. Beconcini ML. Un metodo pratico per la determinazione del tiro nelle catene (A practical method for determining the tension in chains - in Italian). *Costruire in laterizio* 1996; 54: 299–301.

3. Blasi C and Sorace S. Determining the Axial Force in Metallic Rods. *Structural Engineering International* 1994; 4(4): 241–246. DOI:10.2749/101686694780601809.

4. Bati SB and Tonietti U. Experimental Methods for Estimating In Situ Tensile Force in Tie-Rods. *Journal of Engineering Mechanics* 2001; 127(12): 1275–1283. DOI: 10.1061/(ASCE)0733-9399(2001)127:12(1275).

5. Dardano D, Miranda JC, Persichetti B et al. Un metodo per la determinazione del tiro nelle catene mediante identificazione dinamica (A method for the determination of tension in chains through dynamic identification - in Italian). In *Proceedings of the 11th National conference Prove non Distruttive, Monitoraggio e Diagnostica*. Milan.

6. Lagomarsino S and Calderini C. The dynamical identification of the tensile force in ancient tie-rods. *Engineering Structures* 2005; 27(6): 846–856. DOI: 10.1016/j.engstruct.2005.01.008.

7. Park S, Choi S, Oh ST et al. Identification of the tensile force in high-tension bars using modal sensitivities. *International Journal of Solids and Structures* 2006; 43(10): 3185–3196. DOI:10.1016/j.ijsolstr.2005.06.089.

8. Tullini N and Laudiero F. Dynamic identification of beam axial loads using one flexural mode shape. *Journal of Sound and Vibration* 2008; 318(1-2): 131–147. DOI: 10.1016/j.jsv.2008.03.061.

9. Amabili M, Carra S, Collini L et al. Estimation of tensile force in tie-rods using a frequency-based identification method. *Journal of Sound and Vibration* 2010; 329(11): 2057–2067. DOI:10.1016/j.jsv.2009.12.009.

10. Garziera R, Amabili M and Collini L. A hybrid method for the nondestructive evaluation of the axial load in structural tie-rods. *Nondestructive Testing and Evaluation* 2011; 26(02): 197–208. DOI:10.1080/10589759.2011.556728.

11. Gentilini C, Marzani A and Mazzotti M. Nondestructive characterization of tie-rods by means of dynamic testing, added masses and genetic algorithms. *Journal of Sound and Vibration* 2013; 332(1): 76–101. DOI:10.1016/j.jsv.2012.08.009.

12. Li S, Reynders E, Maes K et al. Vibration-based estimation of axial force for a beam member with uncertain boundary conditions. *Journal of Sound and Vibration* 2013; 332(4): 795–806. DOI:10.1016/j.jsv.2012.10.019.

13. Rebecchi G, Tullini N and Laudiero F. Estimate of the axial force in slender beams with unknown boundary conditions using one flexural mode shape. *Journal of Sound and Vibration* 2013; 332(18): 4122–4135. DOI:10.1016/j.jsv.2013.03.018.

14. Campagnari S, di Matteo F, Manzoni S et al. Estimation of Axial Load in Tie-Rods Using Experimental and Operational Modal Analysis. *Journal of Vibration and Acoustics* 2017; 139(4): 1–15. DOI:10.1115/1.4036108.

15. Coïsson E, Collini L, Ferrari L et al. Dynamical Assessment of the Work Conditions of Reinforcement Tie-Rods in Historical Masonry Structures. *International Journal of Architectural Heritage* 2019; 13(3): 358–370. DOI:10.1080/15583058.2018.1563231. URL https://doi.org/10.1080/15583058.2018.1563231.

16. Gentile C, Poggi C, Ruccolo A et al. Vibration-Based Assessment of the Tensile Force in the Tie-Rods of the Milan Cathedral. *International Journal of Architectural Heritage* 2019; 13(3): 411–424. DOI:10.1080/15583058.2018.1563235.

17. Gentile C, Ruccolo A and Canali F. Long-term monitoring for the condition-based structural

maintenance of the Milan Cathedral. *Construction and Building Materials* 2019; 228: 117101. DOI:10.1016/j.conbuildmat.2019.117101. URL https://linkinghub.elsevier.com/retrieve/pii/S0950061819325437.

18. Duvnjak I, Ereiz S, Damjanović D et al. Determination of Axial Force in Tie Rods of Historical Buildings Using the Model-Updating Technique. *Applied Sciences* 2020; 10(17): 6036. DOI:10.3390/app10176036.

19. Belluzzi O. *Scienza delle Costruzioni (Vol.4) (Construction Science - in Italian)*. Nicola zan ed. Bologna, 1955.

20. Cescatti E, da Porto F, Modena C et al. Ties in historical constructions: Typical features and laboratory tests. In *Structural Analysis of Historical Constructions: Anamnesis, Diagnosis, Therapy, Controls*. CRC Press. ISBN 9781315616995, pp. 1301–1307. DOI:10.1201/9781315616995-176.

21. Cescatti E, Da Porto F and Modena C. Axial Force Estimation in Historical Metal Tie-Rods: Methods, Influencing Parameters, and Laboratory Tests. *International Journal of Architectural Heritage* 2019; 13(3): 317–328. DOI:10.1080/15583058.2018.1563234.

22. Nielsen MA. *Neural Networks and Deep Learning*. Determination Press, 2015. URL http://neuralnetworksanddeeplearning.com/index.html.

23. Wang N, Zhao X, Zhao P et al. Automatic damage detection of historic masonry buildings based on mobile deep learning. *Automation in Construction* 2019; 103: 53–66. DOI:10.1016/j.autcon.2019.03.003. URL https://linkinghub.elsevier.com/retrieve/pii/S0926580518307568.

24. Mishra M. Machine learning techniques for structural health monitoring of heritage buildings: A state-of-the-art review and case studies. *Journal of Cultural Heritage* 2021; 47: 227–245. DOI:10.1016/j.culher.2020.09.005.

25. Standoli G, Giordano E, Milani G et al. Model Updating of Historical Belfries Based on Oma Identification Techniques. *International Journal of Architectural Heritage* 2021; 15(1): 132–156. DOI:10.1080/15583058.2020.1723735.

26. Worden K and Manson G. The application of machine learning to structural health monitoring. *Philosophical Transactions of the Royal Society A: Mathematical, Physical and Engineering Sciences* 2007; 365(1851): 515–537. DOI:10.1098/rsta.2006.1938.

27. Hagan MT, Demuth HB, Beale MH et al. *Neural Network Design*. PWS Publishing Co., 1996. ISBN 0971732116.

28. Makoond N, Pelà L and Molins C. Dynamic elastic properties of brick masonry constituents. *Construction and Building Materials* 2019; 199: 756–770. DOI:10.1016/j.conbuildmat.2018.12.071.

29. DIANA FEA. DIANA FEA User's Manual Release 10.4, 2016. URL https://dianafea.com/manuals/d104/Diana.html.

30. Saloustros S, Pelà L, Contrafatto FR et al. Analytical Derivation of Seismic Fragility Curves for Historical Masonry Structures Based on Stochastic Analysis of Uncertain Material Parameters. *International Journal of Architectural Heritage* 2019; 13(7): 1142–1164. DOI:10.1080/15583058.2019.1638992.

31. Baughman D and Liu Y. Fundamental and Practical Aspects of Neural Computing. In *Neural Networks in Bioprocessing and Chemical Engineering*. Elsevier, 1995. pp. 21–109. DOI:10.1016/B978-0-12-083030-5.50008-4.

32. Hagan M and Menhaj M. Training feedforward networks with the Marquardt algorithm. *IEEE Transactions on Neural Networks* 1994; 5(6): 989–993. DOI:10.1109/72.329697. URL http://ieeexplore.ieee.org/document/329697/.

33. Garcia Ramonda L, Isalberti F, Garcia Roca I et al. MSc SAHC SA7 PROJECT: Structural evaluation and safety assessment of the monastery's church of Sant Cugat del Vallès, 2015.

34. Makoond N, Pelà L, Molins C et al. Automated data analysis for static structural health monitoring of masonry heritage structures. *Structural Control and Health Monitoring* 2020; 27(10). DOI:10.1002/stc.2581.

35. PROCEQ. PUNDIT PL-200 Operating Instructions, 2014.

36. Peeters B. *System Identification and Damage Detection in Civil Engineering*. Phd thesis, KU Leuven, 2000. URL https://www.researchgate.net/publication/238331491.

37. Reynders E, Schevenels M and De Roeck G. MACEC 3.2 User's Manual. Technical Report February, 2011. URL https://bwk.kuleuven.be/bwm/macec.

38. MathWorks. MATLAB R2018b Documentation, 2018. URL https://www.mathworks.com/help/releases/R2018b/index.html.

39. Olden JD, Joy MK and Death RG. An accurate comparison of methods for quantifying variable importance in artificial neural networks using simulated data. *Ecological Modelling* 2004; 178(3-4): 389–397. DOI:10.1016/j.ecolmodel.2004.03.013.

40. Olden JD and Jackson DA. Illuminating the "black box": a randomization approach for understanding

variable contributions in artificial neural networks. *Ecological Modelling* 2002; 154(1-2): 135–150. DOI: 10.1016/S0304-3800(02)00064-9. URL https://doi.org/10.1016/S0304-3800(02)00064-9.

41. Sambasivan N, Kapania S, Highfill H et al. "Everyone wants to do the model work, not the data work": Data Cascades in High-Stakes AI. In *Proceedings of the 2021 CHI Conference on Human Factors in Computing Systems.* New York, NY, USA: ACM. ISBN 9781450380966, pp. 1–15. DOI:10.1145/3411764.3445518.